Radiated field of rotating charged parallel plates and its frequency spectrum

Cite as: AIP Advances **8**, 025325 (2018); https://doi.org/10.1063/1.5021638
Submitted: 06 January 2018 • Accepted: 20 February 2018 • Published Online: 28 February 2018

Zongxin Wang, Zhenxin Cao and Fei Yang

Radiated field of rotating charged parallel plates and its frequency spectrum

Zongxin Wang,[a] Zhenxin Cao, and Fei Yang
State Key Laboratory of Millimeter Waves, Southeast University, Nanjing 210096, China

(Received 6 January 2018; accepted 20 February 2018; published online 28 February 2018)

Antennas in the ultra low frequency (ULF, 300 Hz to 3 kHz) and very low frequency (VLF, 3~30 kHz) bands are usually very large. In this study, we developed a very small antenna, which can radiate electromagnetic waves in these frequency bands. The antenna consisted of two rotating charged plates (RCPs), which were charged by the voltage source. Numerical results of the radiated far field and its frequency spectrum are presented for three cases: (a) the antenna is charged with DC voltage, (b) the antenna is charged with AC voltage, and (c) the antenna rotates with variable speed and is fed with DC voltage. The predominant frequency component was equal to the rotating frequency of the RCPs fed with DC voltage. If the RCPs were fed with AC voltage two dominant frequencies were generated, which were determined by the difference in frequency between the RCP rotation frequency and the AC source frequency. When the RCPs rotated with variable speed and were fed with DC voltage, many frequency components were generated, which were determined by the initial rotational speed of the RCPs and their acceleration. https://doi.org/10.1063/1.5021638

I. INTRODUCTION

The frequency spectrum of the low frequency electromagnetic wave is used in a large number of military applications. The most important benefit of the ultra low frequency (ULF, frequency range 300 Hz to 3 kHz) signal is that it can penetrate conductive media such as sea water[1] and is suitable for underwater military communications. The very low frequency (VLF, frequency range of 3~30 kHz) is also suitable for military communication. VLF electromagnetic waves can propagate in the earth-ionosphere waveguide and can travel long distances, enabling over-horizon-communication. Free space wavelengths may reach hundreds to thousands of kilometers at ULF and VLF frequencies. The commonly designed antennas in these frequencies are extremely large and impractical in many operational environments. Recently, new types of ULF and VLF antennas, which use the physical motion of an electret(or magnet) to generate electromagnetic waves have been developed. These antennas are called mechanical (or spinning) antennas.[2–4]

It is known that electric and magnetic fields induce each other in turn to form electromagnetic waves that can be transmitted. When an electric charge makes a specific movement, the electric field produced by the moving charge varies in space, and then induces the magnetic field, which is mutually inductive to the electric field; thus, an electromagnetic wave is generated and radiated.

Based on this concept, rotating charges can be used as an antenna in the ULF and VLF bands. The volume of this rotating mechanical antenna would be much smaller than those designed by the conventional method. In this study, we developed an antenna that consisted of two rotating parallel conductor plates, which were charged by the voltage source. As with all mechanical (or spinning) antennas, the far field radiation efficiency of the rotating charged plates (RCP) antenna was almost irrelevant to its size. Therefore, the RCPs could be designed with a reasonable and practical

[a]wangzx@seu.edu.cn

size, for example 1×1×1m, while the radiation efficiency of a 1m scale conventional VLF antenna (for example a dipole at 10kHz) is less than 1×10^{-12} and is impractical for transmitting to the far field.[2]

II. THEORY

The radiation electric field and magnetic field produced by a low velocity charge[5] can be expressed with equation (1) and equation (2).

$$\mathbf{E} = \frac{q}{4\pi\varepsilon_0 c^2 r^3}\boldsymbol{r}\times(\boldsymbol{r}\times\dot{\boldsymbol{v}}) \tag{1}$$

$$\mathbf{B} = \frac{q\dot{\boldsymbol{v}}\times\boldsymbol{r}}{4\pi\varepsilon_0 c^3 r^2} \tag{2}$$

Where q is the amount of the charge, $\boldsymbol{r}$ is the radius vector of the charge to the far zone field, $\boldsymbol{v}$ and $\dot{\boldsymbol{v}}$ are the velocity and the acceleration of the charge respectively,c is the speed of light, and ε_0 is the permittivity of a vacuum.

From equations (1) and (2), we know that the moving charge, even if its speed is very low, can radiate electromagnetic waves as long as it has acceleration. Figure 1 shows that for a pair of parallel plates with $2r_0$ spacing and positive and negative electrodes attached to the two plates, the positive and negative charges will be aggregated on the two conductor plates. When the two conductor plates rotate around the axis (Z axis),the charge will have normal acceleration, thus radiating the electromagnetic wave.

Assuming that the charge is evenly distributed on the plate (the charge density is ρ), the radiation field at a point P produced by the charge on the positive electrode plate is as follows:

$$\mathbf{E} = \iint_s \frac{\rho}{4\pi\varepsilon_0 c^2 r^3}\boldsymbol{r}\times(\boldsymbol{r}\times\dot{\boldsymbol{v}})ds \tag{3}$$

The charge quantity on the negative plate isthe same as that on the positive plate, but the acceleration direction of the points on the negative plate is the opposite of the acceleration direction of the corresponding point on the positive plate. According to equation (1), and taking into account that the distance between the two plates is far less than their distance to the far field point, the radiation field generated by the negative and positive charges is approximately equal. The radiation electric fields

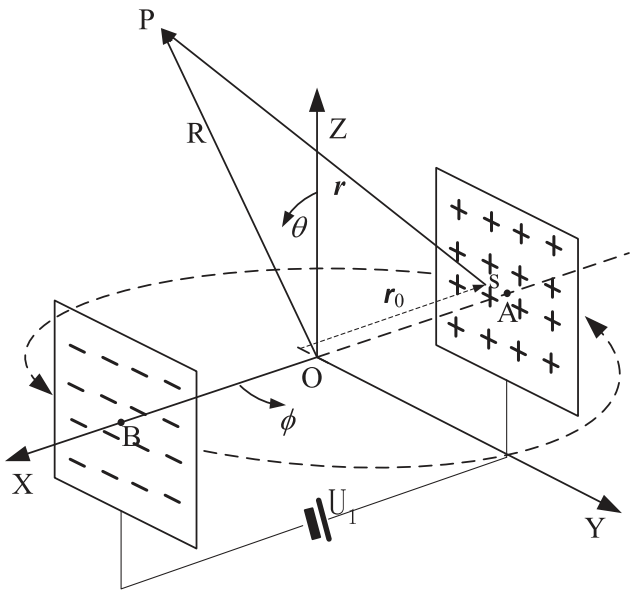

FIG. 1. Construction of the rotating charged parallel plate.

generated by the rotating parallel plates in the far zone are:

$$\mathbf{E} = \iint_s \frac{2\rho}{4\pi\varepsilon_0 c^2 r^3} \boldsymbol{r} \times (\boldsymbol{r} \times \dot{\boldsymbol{v}}) ds \tag{4}$$

For a rotating point, the normal acceleration can be represented by the angular velocity of rotation:

$$\dot{v} = \omega^2 r_0 \tag{5}$$

where ω is the angular velocity and r_0 is the distance between the charge and the rotation axis.

III. NUMERICAL RESULTS

Setting the plate size as 30×30mm, the distance between the two plates as 100mm, and the rotational speed as 500 revolutions per second (r.p.s.) ($\omega = 2\pi \times 500$),the electric fields of the RCPs are computed according to equation (4). The numerical results of the normalizedelectric field (at a moment when the axis of the two plates (line AB) is rotated coinciding with the x-axis) are given in Figure 2. The 3-D view of the x-polarized electric field (Ex) looks like a rolling tire along the x-axis, and theamplitude of Ey (y-polarized electric field) and Ez (z-polarized electric field), respectively, are far less than that of Ex. The 2-D curves of the electric fields (Ex, Ey, and Ez) in two orthogonal planes are shown in Figure 3, which shows the details of the electric field. A 3-D view of the normalized magnetic field is given in Figure 4. The x-polarized magnetic field is almost zero in this situation and is not shown.

The actual amplitudes of the radiated fields of the RCPs depended on the amount of charge gathered on the plates. The voltage could be increased by various methods (for example, by adding a static conductor ring ribbon around the rotating plates and adding a high dielectric constant material between them) to increase the amount of charge. A 1×1mm rotating plate (radius of rotation r_0=1m) charged with a 250-kV voltage was able to generate an electric field strength of up to 10^{-7}~10^{-8}V/m in the ionosphere 70 km away. This electromagnetic wave could then propagate in the earth-ionosphere

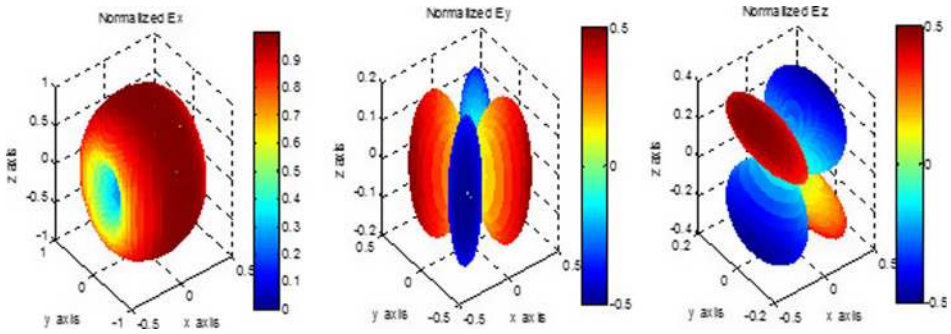

FIG. 2. Radiated electric field of the rotating charged plates (RCPs) (the positive plate at coordinate (30mm, 0, 0)).

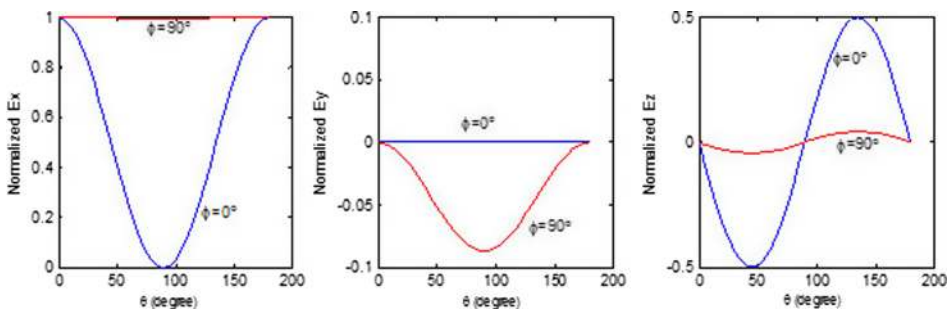

FIG. 3. 2-D Radiated electric field of the rotating charged plates (RCPs) (the positive plate at coordinate (30mm, 0, 0))

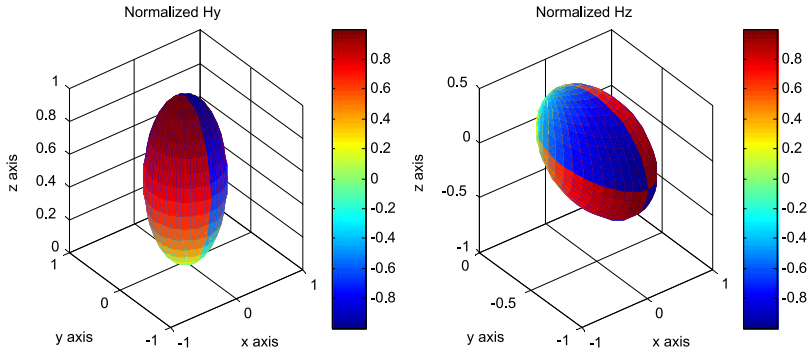

FIG. 4. Radiated magnetic field of the rotating charged plates (RCPs) (the positive plate at coordinate (30mm, 0, 0)).

wave-guide, with little attenuation and could be easily received by ground equipment. To generate an electromagnetic wave of the same strength at a distance of 60 km with a dipole, the length of the dipole metal wire would need to be in the magnitude of kilometers.

The working frequency is an important parameter of electric equipment, and therefore we analyzed the frequency spectrum of the radiated electromagnetic waves of the RCPs. The far field could be computed at any specific point according to equation (4) and the fields were recorded in the time domain while the plates rotated. A Fast-Fourier-Transform (FFT)[6] was then performed to obtain the frequency spectrum. The frequency spectrum was analyzed for three cases: (a) the antenna is charged with DC voltage, (b) the antenna is charged with AC voltage, (c) the antenna rotates with variable speed and is fed with DC voltage.

(a) The antenna is charged with DC voltage

The predominant frequency component of the DC voltage-charged RCPs was determined by its rotating frequency. The rotating speed of the RCPs was set to 500r.p.s. and its far field was computed. Figure 5 shows the Ex field of the RCPs in the time domain and its frequency spectrum. The predominant frequency component, f_0, was 500Hz, which was equal to the rotating frequency of the RCPs. The same frequency spectrum was obtained using Ey or Ez.

(b) The antenna is charged with AC voltage

If the RCPs are charged with AC voltage, the charge on the plates can be expressed as:

$$q(t) = qsin(2\pi f_1 t) \tag{6}$$

where q is the maximum amount of charge and f_1 is the frequency of the AC voltage.

The rotating speed of the RCPswas again set to 500r.p.s. and its far field was computed. The numerical results when $f_1 = 2f_0$ and $f_1 = 0.5f_0$ are shown in Figures 6 and 7, which show that two dominant frequencies were generated: $f_1 + f_0$ and $|f_1 - f_0|$.

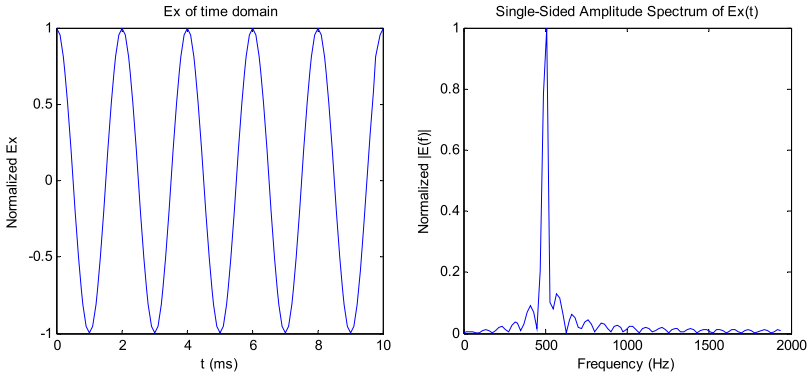

FIG. 5. The radiated field (observed at a far zone point) of the rotating charged plates (RCPs) charged with DC voltage.

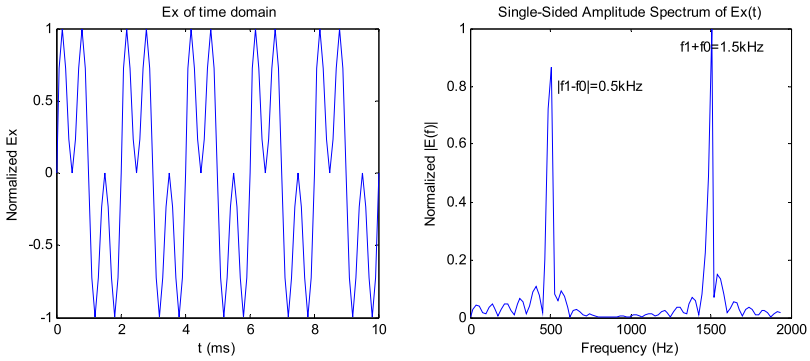

FIG. 6. Far field (observed at a far zone point) frequency spectrum when the AC frequency $f_1 = 2f_0$.

(c) The antennarotates with variable speed and is fed with DC voltage

Figure 8 assumes that the RCPs start to rotate from point A, with an initial angular velocity $\omega_0 = 2\pi N_0(N_0\text{-r.p.s.})$, are uniformly accelerated with acceleration ω' in a period of time t, and move to point B (speed up to an angular velocity ω_1). In the next period of time t the RCPs decelerate evenly, with deceleration ω' to the original angular velocity ω_0 and move to point C. We call this time period, where the RCP rotates from point A to C, a varying velocity period (VVP), which includes one acceleration time interval (from point A to point B) and one deceleration time interval (from point B to point C).

In the acceleration interval, the instantaneous angular velocity of the RCPs is $\omega_0 + \omega' t$ and the acceleration time length t_a can be obtained by equation (7).

$$\int_0^t (\omega_0 + \omega'\tau)d\tau = \phi_0 \tag{7}$$

The solution of equation (7) is easily obtained as:

$$t_a = -\frac{\omega_0}{\omega'} + \sqrt{\left(\frac{\omega_0}{\omega'}\right)^2 + \frac{2\phi_0}{\omega'}} \tag{8}$$

For the observed far field, only when the RCPs were back to point A and their velocity and acceleration returned to the original value when it started from A, was a cycle completed. We called this cycle the far-field-cycle (FFC). To complete a FFC, the RCPs needed to rotate by at least one revolution. In cases when the RCPs rotated by more than one revolution to finish a FFC, only one VVP was completed (i.e., more than one revolution is needed to increase the speed of the RCP to

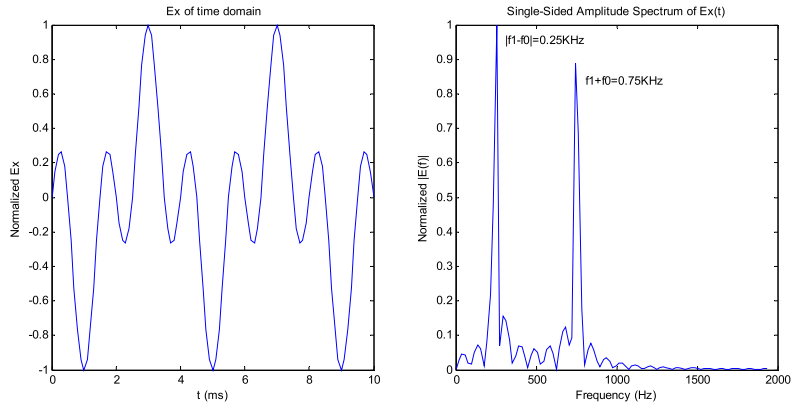

FIG. 7. Far field frequency spectrum when the AC frequency $f_1 = 0.5f_0$.

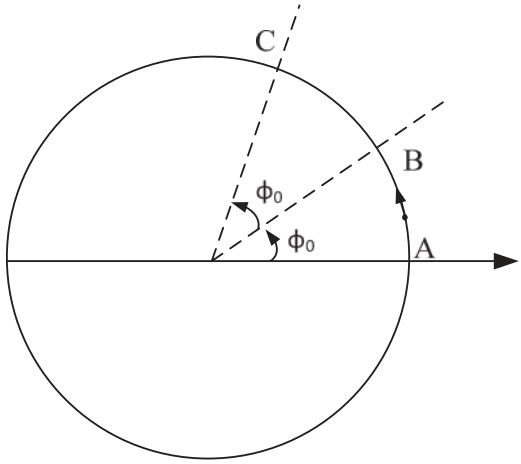

FIG. 8. Rotating charged plates (RCPs) movement cycle.

ω_1). For simplicity, ϕ_0 is determined as:

$$\phi_0 = \frac{2n\pi}{2m} = \frac{n\pi}{\mathrm{m}} \tag{9}$$

where m and n are both integers greater than or equal to 1, m represents the number of VVPs passed in one FFC, and n represents the number of revolutions in one FFC.

Usually, the RCPs are driven by an electric motor, and they need to be rotated by many revolutions to reach an appreciable rotation velocity. In practice, m=1 and n>1 are usually selected, otherwise a very large acceleration ω′ is needed. For example, if m=5 and n=1were selected, five VVPs would need to be completed after the RCPs completed one revolution (impossible for a real motor, possible for an electron in an accelerator).

For numerical implementation, the values of m, n, and ω' were set, ϕ_0 and t_a were calculated according to equations (9) and (8) successively, and the far field was calculated at the observation point using equation (4), taking note of the angular velocity ω in each VVP,as shown in equation (10).

$$\begin{cases} \omega(t) = \omega_0 + \omega' t & t < t_a \\ \omega(t) = \omega_0 + 2\omega' t_a - \omega' t & t_a < t < 2t_a \end{cases} \tag{10}$$

The numerical results of parameter setting NO.1 (N_0=280 r.p.s., m=1, n=200, ω′ =750rad/s^2) are given in Figure 9, including Ex of the time domain (only one FFC for clarity) and its frequency spectrum. With parameter setting NO.1, the rotational speed of the RCPs increased to N_1=300 r.p.s. at the end of an acceleration interval. It is clear that many frequency components were generated around the N_0~N_1 region.

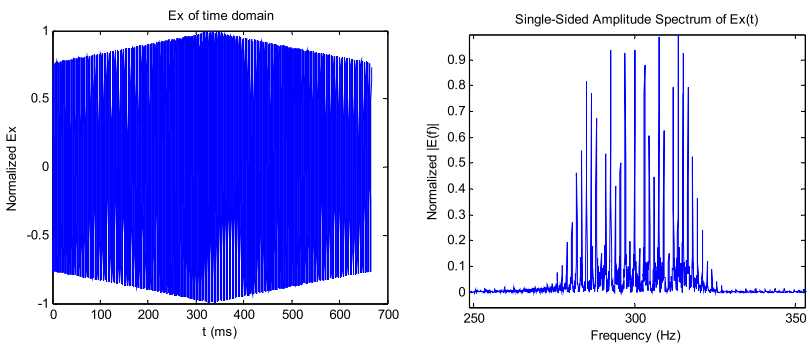

FIG. 9. Frequency spectrum of the far field (parameter setting NO.1).

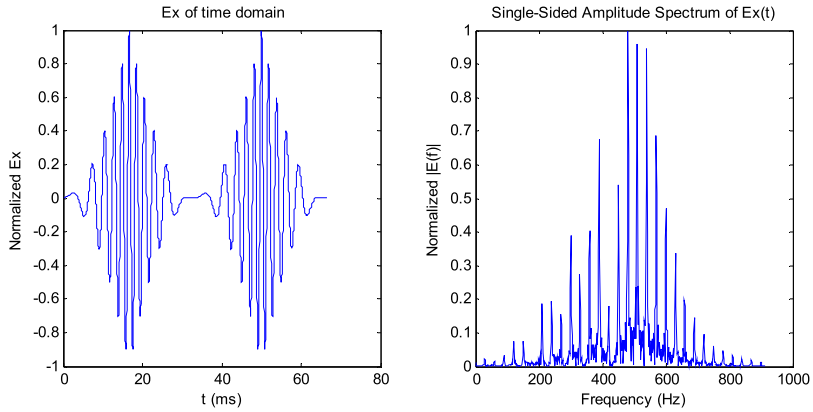

FIG. 10. Frequency spectrum of the far field (parameter setting NO.2).

The numerical results of parameter setting NO.2 (N_0=10r.p.s., m=1, n=10, $\omega' = 11000 rad/s^2$, the rotational speed of the RCP was increased to N_1=300 r. p.s.) are given in Figure 10. Although the acceleration ω' is so large, it is not practical for a real motor; the example has theoretical value. From Figure 10, it can be seen that if the acceleration is large enough, higher (than the fastest revolution speed) frequency components can be obtained.

IV. CONCLUSION

Avery small antenna for radiating ULF and VLF bands was developed in this study. This antenna consisted of two rotating parallel conductor plates, which were connected to a voltage source. The far field of the antenna and itsfrequency spectrums were analyzed. The numerical results showed that the predominant frequency component was equal to the rotation frequency of the RCPs if it was fed with a DC voltage. Alternatively,if the RCP was fed with an AC voltage two dominant frequencies were generated, which were determined by the difference in frequency between the rotation frequency of the RCPs and the AC source frequency. In another case, the RCPs were rotated with variable speed and fed with DC voltage, which generated many frequency components that were determined by the initial rotational speed of the RCPs and its acceleration.

ACKNOWLEDGMENTS

This work is supported by the National Natural Science Foundation of China under grants 61471117 and 61101020.

[1] D. L. Hershberger, "Wideband VLF and LF systems," 2017 IEEE Symposium on Antennas and Propagation, San Diego, California, 9–14 July, 2017 (IEEE Antennas and Propagation Society), pp. 1479–1480.
[2] J. A. Bickford, R. S. McNabb, P. A. Ward, D. K. Freeman, and M. S. Weinberg, "Low frequency mechanical antennas," 2017 IEEE Symposium on Antennas and Propagation, San Diego, California, 9–14 July, 2017 (IEEE Antennas and Propagation Society), pp. 1475–1476.
[3] M. Manteghi, "A navigation and positioning system for unmanned underwater vehicles based on a mechanical antenna," 2017 IEEE Symposium on Antennas and Propagation, San Diego, California, 9–14 July, 2017 (IEEE Antennas and Propagation Society), pp. 1997–1998.
[4] S. Selvin, M. N. Srinivas Prasad, Y. Huang, and E. Wang, "Spinning magnet antenna for VLF transmitting," 2017 IEEE Symposium on Antennas and Propagation, San Diego, California, 9–14 July, 2017 (IEEE Antennas and Propagation Society), pp. 1477–1478.
[5] J. D. Jackson, *Classical Electrodynamics*, Third Edition (John Wiley & Sons Inc, 1998), pp. 661–665.
[6] Matlab User's Guide, Mathworks Inc., 2010.